Nanoscale Advances

ROYAL SOCIETY OF CHEMISTRY

COMMUNICATION

View Article Online
View Journal | View Issue

Cite this: *Nanoscale Adv.*, 2020, **2**, 1427

Received 23rd December 2019
Accepted 16th February 2020

DOI: 10.1039/c9na00796b

rsc.li/nanoscale-advances

Giant ultrafast optical nonlinearities of annealed Sb_2Te_3 layers†

Charles Moisset,[a] Richard-Nicolas Verrone,[a] Antoine Bourgade,[a] Gebrehiwot Tesfay Zeweldi,[a] Marco Minissale,[b] Laurent Gallais,[a] Carine Perrin-Pellegrino,[c] Hassan Akhouayri,[a] Julien Lumeau,[a] Jean-Yves Natoli[a] and Konstantinos Iliopoulos *[a]

The optimization of thin Sb_2Te_3 films in order to obtain giant ultrafast optical nonlinearities is reported. The ultrafast nonlinearities of the thin film layers are studied by the Z-scan technique. Giant saturable absorption is obtained, which is the highest ever reported, by means of the Z-scan technique.

There is a growing interest in materials exhibiting significant ultrafast nonlinear optical (NLO) properties.[1] In particular, the saturable absorption is currently intensively being investigated because it can be directly applied to the mode-locking of laser systems.[2] Many different materials, for example, carbon nanotubes,[3] graphene[4] and perovskites[5,6] have been reported in the past to exhibit a significant saturable absorption.

Moreover, nowadays, intense research is being carried out in the field of nano-patterning materials in order to offer them unique optical/nonlinear optical properties.[7] This has a strong impact in many applications, for example, optical filtering,[8,9] diffractive element fabrication[10] and optical data storage,[11] to name a few. The direct laser writing technique,[12] using fs laser pulses, is one of the most promising and cost-efficient techniques used in order to pattern the matter with custom shapes. However, the resolutions are usually limited by diffraction. The latter can be surpassed by nonlinear phenomena, but the resolutions obtained are very highly dependent on the material used for patterning.[13,14] An improved way to surpass the diffraction limit is to use a super-resolution mask exhibiting a significant saturable absorption.[15]

A family of 2D materials, called topological insulators, exhibiting a "graphene-like" energy band gap structure, is currently very intensively being investigated, as these materials exhibit very high optical nonlinearities.[16,17] Among them, Sb_2Te_3 is currently among the best candidates for the mode-locking of ultrafast laser systems.[18,19] Despite the high interest of this material for photonic applications, its NLO parameters at the ultrafast regime, are rather unknown. There is currently only one study reporting on the nonlinear absorption coefficient (β) of Sb_2Te_3 using ultrafast pulses.[20] An optimization of its NLO response is very complex because it highly depends on its crystallization state. Research on this topic is of high interest because it will further enhance the applicability of Sb_2Te_3 in the field of photonics.

Our group is aiming at using thin Sb_2Te_3 layers as super-resolution masks in the ultrafast regime. Towards this objective, a thorough optimization of the crystallization state of Sb_2Te_3 thin films was initiated in order to obtain an optimal saturable absorption. In this work deposition, post treatment and NLO studies are presented. The crystallization was done by oven and laser annealing. In both cases, unprecedented nonlinear absorption parameters have been found, which are compared with state-of-the-art materials.

The Sb_2Te_3 thin films were deposited using the electron beam deposition technique. The thickness of the films has been determined to be 24 nm, by locally removing the thin layer and performing atomic force microscopy measurements (Fig. S1†). A 10 nm thick silica layer was deposited over Sb_2Te_3, which allowed us to perform annealing in air without the oxidation of the layers. The substrate and the thin silica layer have been found to exhibit no optical nonlinearities under the experimental conditions used in this work.

After the deposition, annealing was performed in two different ways. Firstly, the thin films were annealed by using an oven at 300 °C for 24 hours, following a procedure previously reported by our group.[21] A second alternative way to crystallize the thin films has been employed in this work. In this case, laser annealing was performed by using a pump-probe setup (Fig. S2 and description in the ESI†).[22] During laser annealing the temperature on the sample was *in situ* measured by using a thermal camera throughout crystallization. Moreover, the relative reflectance, which is well-known to be strongly dependent upon the crystallization state of the Sb_2Te_3 material,[23] was

[a]*Aix Marseille Univ, CNRS, Centrale Marseille, Institut Fresnel, Marseille, France. E-mail: konstantinos.iliopoulos@fresnel.fr*

[b]*Aix Marseille Univ, CNRS, PIIM, Marseille, France*

[c]*Aix Marseille Univ, Univ Toulon, CNRS, IM2NP, UMR 7334, Marseille, France*

† Electronic supplementary information (ESI) available. See DOI: 10.1039/c9na00796b

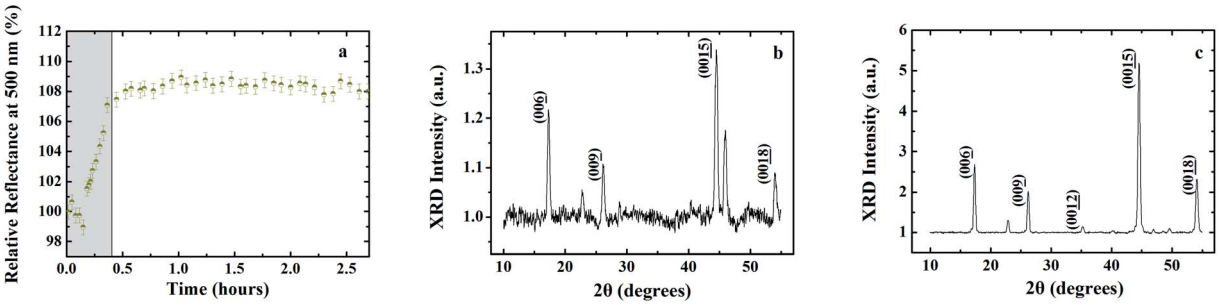

Fig. 1 (a) Relative reflectivity at 500 nm as a function of the annealing time. (b) XRD diagram of the laser annealed sample. (c) XRD diagram of the oven annealed sample.

measured in the 500 nm to 1000 nm wavelength range, throughout the procedure, in order to provide a precise control of annealing. In Fig. S3†, relative reflectance spectra are presented for different annealing times. In Fig. 1a, the relative reflectance at 500 nm is shown, as a function of the annealing time. The gray part of the graph corresponds to the temperature increasing zone. In this part of the graph there is an initial decrease of the reflectance, which we attribute to a modification of the refractive index with temperature. Then a gradual increase is observed, which is attributed to the increase of the crystalline volume fraction of the thin film layers. The maximum temperature employed in order to acquire optimal crystallization is 350 °C. It can be seen that the relative reflectance reaches a maximum after about 45 minutes of annealing, while it remains unchanged for longer crystallization times, revealing that overall crystallization has been achieved.

UV-Vis spectrophotometric studies have been additionally performed for all the annealed and amorphous samples. Moreover, the refractive indices have been determined by using a single oscillator using the Drude modified Forouhi–Bloomer model. The spectra and the refractive index values have been found to be in very good agreement with previous results reported by our group.[21]

X-Ray diffraction (XRD) studies were then performed for the crystallized samples. Representative XRD diagrams can be seen in Fig. 1(b and c) for the laser annealed and oven annealed samples respectively. These results are in very good accordance with previous crystallographic studies of the Sb_2Te_3 material.[21,24–26] The difference of the peak amplitudes is attributed to the different annealing surfaces. In the case of oven annealing the whole sample surface was annealed, while in the case of laser annealing a surface area of approximately 1 cm^2 was crystallized. The positions of the diffraction peaks are very similar in both cases, indicating very similar crystalline structures. The main peaks of XRD diagrams are attributed to the Sb_2Te_3 rhombohedral structure, with a 00*l* preferred orientation.[21,27] The additional peaks appearing at about 22.8 and 45.9 degrees, the latter only in the case of laser annealing, can probably be attributed to Te.[28] This difference does not seem to affect the NLO response, which has been found to be very similar for both annealing procedures.

The NLO response of the samples was measured by means of the Z-scan technique[29,30] (Fig. S4 and short description in the ESI†), employing 600 fs laser pulses using IR (1030 nm) and visible (515 nm) laser excitation with a 10 Hz repetition rate. The nonlinear refraction of the thin films studied in this work has been found to be negligible compared with the nonlinear absorption under the same experimental conditions. In Fig. 2 representative "open aperture" Z-scan curves for the oven annealed films using 1030 nm and 515 nm laser excitation wavelengths are presented. Similar results have been obtained in the case of the laser annealed samples (Fig. S5†). The amorphous samples exhibited negligible NLO responses under the same

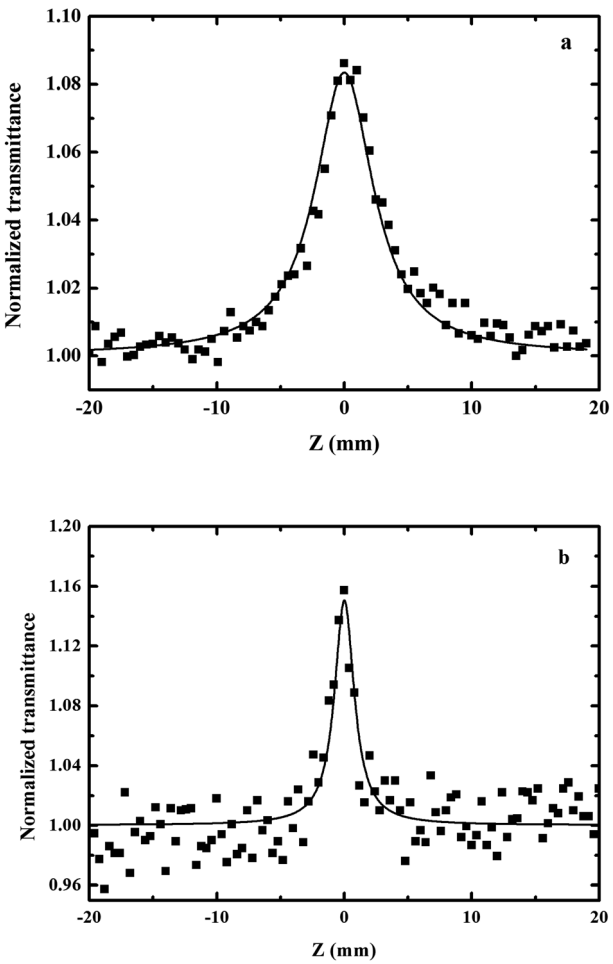

Fig. 2 Representative "open-aperture" Z-scan curves obtained for the oven annealed samples using 600 fs laser pulses at (a) 1030 nm, $I = 2$ GW cm^{-2} and (b) 515 nm, $I = 2$ GW cm^{-2}.

Table 1 Nonlinear optical parameters determined in this work and comparison with state-of-the-art saturable absorbers

Material	Experimental parameters	β [cm GW^{-1}]	Im$\chi^{(3)}$ [$\times 10^{-11}$ esu]	Ref.
Bi_2Se_3	800 nm, 1 kHz, 65 fs	−596 980	N/A	39
Sb_2Te_3 (oven annealing)	515 nm, 10 Hz, 600 fs	−380 000	−15 000	This work
Sb_2Te_3 (laser annealing)	515 nm, 10 Hz, 600 fs	−340 000	−14 000	This work
$(BA)_2(MA)Pb_2I_7$	570 nm, 150 fs	−256 000	N/A	40
Sb_2Te_3 (oven annealing)	1030 nm, 10 Hz, 600 fs	−200 000	−39 000	This work
Sb_2Te_3 (laser annealing)	1030 nm, 10 Hz, 600 fs	−200 000	−39 000	This work
2D α-Mo_2C	1550 nm, 2 kHz	−100 000	N/A	32
$GeSb_4Te_7$	800 nm, 1 kHz, 100 fs	−93 009	N/A	33
Carbon nanotubes	1300 nm, 1 kHz, 200 fs	N/A	−8500	3
Bi_2Se_3	800 nm, 2 kHz, 35 fs	−65 000	−1770	34
Bi_2Te_3	1050 nm, 2 kHz, 35 fs	−47 000	−1720	34
Sb_2Te_3	800 nm, 1 kHz, 100 fs	−37 100	N/A	20
WS_2	515 nm, 1 kHz, 340 fs	−29 000	−8440	41
Bi_2Te_2Se	1050 nm, 2 kHz, 35 fs	−25 000	−930	34
Bi_2TeSe_2	1050 nm, 2 kHz, 35 fs	−24 000	−870	34
Black phosphorus	1160 nm, 65 fs	−6980	−4340	37
$CH_3NH_3PbI_3$	800 nm, 80 MHz, 140 fs	−1934	N/A	38
$MAPbI_3$	514 nm, 1 kHz, 200 fs	−1500	N/A	5
MoS_2/graphene	800 nm, 1 kHz	−1217.76	−320	36
Graphene	800 nm, 1 kHz	−961.57	−240	36
WS_2	800 nm, 1 kHz, 40 fs	−397	−178	41
MoS_2	1030 nm, 1 kHz, 340 fs	−250	−150	41
MoS_2	800 nm, 1 kHz	−136.13	−30	36
Graphene	790 nm, 1 kHz, 80 fs	−90	N/A	4
Graphene oxide	790 nm, 1 kHz, 80 fs	−40	N/A	4
$CsPbBr_3$	515 nm, 1 kHz, 340 fs	−0.35	N/A	6

experimental conditions. Thorough measurements were performed in order to verify that no modification of the thin films was induced during the Z-scan studies. This has been achieved by performing studies in a large range of intensities (0.1 GW cm^{-2} to 2.5 GW cm^{-2}) and in many different sample positions, in order to confirm excellent repeatability (Fig. S6 and S7†).

As it can be seen in Fig. 2, a transmission maximum was obtained in all cases around the focal plane, which is due to the strong saturable absorption (SA) character of the thin films. The nonlinearities obtained in this work emanate from the topological insulator-type character of Sb_2Te_3. Indeed, Sb_2Te_3 is well-known to have insulating states in the bulk and "graphene-like" conducting states at its surface. The bleaching of the absorption, which results in a SA attribute, is caused by the Pauli blocking principle.[31]

The "open-aperture" Z-scans obtained in this work have been analyzed using previously published procedures.[28] The nonlinear absorption coefficient and the imaginary part of the third order nonlinear optical susceptibility (Im$\chi^{(3)}$) have been determined by many experimental curves and are presented in Table 1 in the case of the oven and laser annealed samples. The obtained values are of the order of $\beta \sim 10^5$ cm GW^{-1} and Im$\chi^{(3)} \sim 10^{-7}$ esu. These values are the highest ever reported by the Z-scan technique for a saturable absorber. No evidence of nonlinear refraction has been obtained during our measurements. We estimate that the real part of the third order nonlinear optical susceptibility (Re$\chi^{(3)}$) is at least one order of magnitude lower than the imaginary part (Im$\chi^{(3)}$), under the same experimental conditions. In Table 1, a comparison with other state-of-the-art materials is done. The NLO parameters reported here are about one order of magnitude higher compared with a previous study for Sb_2Te_3.[20] They are also 2–4 times higher than those reported for 2D α-Mo_2C crystals,[32] $GeSb_4Te_7$,[33] and carbon nanotubes,[3] 5 times to more than one order of magnitude compared with those of $Bi_2Te_xSe_{3-x}$ materials,[34] 2–4 orders of magnitude higher than the NLO responses reported for graphene and graphene oxide[4,35,36] and 2–3 orders of magnitude higher than those of black phosphorus.[37] The NLO parameters measured in this work are about 6 orders of magnitude higher than those of $CsPbBr_3$ perovskite quantum dots[6] and 2 orders of magnitude higher than those of $MAPbI_3$ perovskites[5] and $CH_3NH_3PbI_3$ perovskite nanosheets.[38] Nonlinear optical parameters of the same order of magnitude with those reported here have been found by Zhang *et al.*[39] in the case of Bi_2Se_3. However the authors employ a different experimental technique (micro P-scan) so a further comparison of the performances is not feasible. Similar values with those found here have been reported by Abdelwahab *et al.* in the case of single-crystalline 2D perovskites, however, in that case a tuning of the excitation wavelength was necessary.[40] On the contrary, the findings reported here show that large values can be obtained for Sb_2Te_3 thin films both in the visible and the IR parts of the spectrum. The broadband NLO character of the thin films optimized in this work reveals a significant advantage of the Sb_2Te_3 material.

Conclusions

In summary, precise crystallization of Sb_2Te_3 thin films has been performed in order to enhance the optical nonlinearities in the IR and visible parts of the spectrum. Large nonlinear

absorption coefficients are obtained ($\sim 10^5$ cm GW^{-1}), which are the highest values ever obtained for a saturable absorber, by means of the Z-scan technique. These results show that this material is a very high performance saturable absorber in the ultrafast regime. The process followed here in order to enhance the optical nonlinearities provides a reference for several fields of photonics, such as mode-locking and super-resolution.

Conflicts of interest

There are no conflicts of interest to declare.

Acknowledgements

This work was supported by the Region PACA (Project: APEX 2017 NANOFAB). The authors also acknowledge support from the Ministry of Armed Forces (DGA) and Aix-Marseille University.

References

1 J. Xu, X. Li, J. Xiong, C. Yuan, S. Semin, T. Rasing and X. Bu, *Adv. Mater.*, 2019, 1806736.
2 D. Mao, B. Du, D. Yang, S. Zhang, Y. Wang, W. Zhang, X. She, H. Cheng, H. Zeng and J. Zhao, *Small*, 2016, **12**, 1489–1497.
3 S. Tatsuura, M. Furuki, Y. Sato, I. Iwasa, M. Tian and H. Mitsu, *Adv. Mater.*, 2003, **15**, 534–537.
4 S. Kumar, M. Anija, N. Kamaraju, K. S. Vasu, K. S. Subrahmanyam, A. K. Sood and C. N. R. Rao, *Appl. Phys. Lett.*, 2009, **95**, 191911.
5 B. S. Kalanoor, L. Gouda, R. Gottesman, S. Tirosh, E. Haltzi, A. Zaban and Y. R. Tischler, *ACS Photonics*, 2016, **3**, 361–370.
6 J. Li, H. Dong, B. Xu, S. Zhang, Z. Cai, J. Wang and L. Zhang, *Photonics Res.*, 2017, **5**, 457–460.
7 J. Lee, M. Tymchenko, C. Argyropoulos, P.-Y. Chen, F. Lu, F. Demmerle, G. Boehm, M.-C. Amann, A. Alù and M. A. Belkin, *Nature*, 2014, **511**, 65–69.
8 T. D. James, P. Mulvaney and A. Roberts, *Nano Lett.*, 2016, **16**, 3817–3823.
9 R. Mudachathi and T. Tanaka, *Sci. Rep.*, 2017, **7**, 1999.
10 N. Yu and F. Capasso, *Nat. Mater.*, 2014, **13**, 139–150.
11 K. Iliopoulos, O. Krupka, D. Gindre and M. Sallé, *J. Am. Chem. Soc.*, 2010, **132**, 14343–14345.
12 M. Beresna, M. Gecevičius and P. G. Kazansky, *Adv. Opt. Photonics*, 2014, **6**, 293–339.
13 S. Juodkazis, V. Mizeikis, K. K. Seet, M. Miwa and H. Misawa, *Nanotechnology*, 2005, **16**, 846–849.
14 R. Wollhofen, J. Katzmann, C. Hrelescu, J. Jacak and T. A. Klar, *Opt. Express*, 2013, **21**, 10831–10840.
15 J. Wei, S. Liu, Y. Geng, Y. Wang, X. Li, Y. Wu and A. Dun, *Nanoscale*, 2011, **3**, 3233–3237.
16 Z. Luo, Y. Huang, J. Weng, H. Cheng, Z. Lin, B. Xu, Z. Cai and H. Xu, *Opt. Express*, 2013, **21**, 29516–29522.
17 H.-R. Chen, C.-Y. Tsai, H.-M. Cheng, K.-H. Lin, P.-H. Yen, C.-H. Chen and W.-F. Hsieh, *Sci. Rep.*, 2016, **6**, 38444.
18 Z. Wang, C. Li, J. Ye, Z. Wang and Y.-G. Liu, *Laser Phys. Lett.*, 2019, **16**, 025103.
19 M. Kowalczyk, J. Bogusławski, R. Zybała, K. Mars, A. Mikuła, G. Soboń and J. Sotor, *Opt. Mater. Express*, 2016, **6**, 2273.
20 C. Liu, L. Cheng, Y. Yuan, J. Su, X. Zhang, X. Li, H. Zhao, H. Zhang, Y. Zheng and J. Li, *Mater. Res. Express*, 2019, **6**, 086446.
21 C. Moisset, A. Bourgade, J. Lumeau, F. Lemarchand, C. Perrin-Pellegrino, H. Akhouayri, J.-Y. Natoli and K. Iliopoulos, *Opt. Mater.*, 2018, **86**, 7–11.
22 M. Minissale, C. Pardanaud, R. Bisson and L. Gallais, *J. Phys. D: Appl. Phys.*, 2017, **50**, 455601.
23 S. Fujimori, S. Yagi, H. Yamazaki and N. Funakoshi, *J. Appl. Phys.*, 1988, **64**, 1000–1004.
24 Q. Wang, B. Liu, Y. Xia, Y. Zheng, R. Huo, M. Zhu, S. Song, S. Lv, Y. Cheng, Z. Song and S. Feng, *Phys. Status Solidi RRL*, 2015, **9**, 470–474.
25 Y. Yin, H. Sone and S. Hosaka, *J. Appl. Phys.*, 2007, **102**, 064503.
26 T. Liu, H. Deng, H. Cao, W. Zhou, J. Zhang, J. Liu, P. Yang and J. Chu, *J. Cryst. Growth*, 2015, **416**, 78–81.
27 PDF # 01-072-1990; ICDD, 2002.
28 PDF # 00-036-1452; ICDD, 2002.
29 M. Sheik-Bahae, A. A. Said, T.-H. Wei, D. J. Hagan and E. W. Van Stryland, *IEEE J. Quantum Electron.*, 1990, **26**, 760–769.
30 K. Iliopoulos, A. El-Ghayoury, H. El Ouazzani, M. Pranaitis, E. Belhadj, E. Ripaud, M. Mazari, M. Sallé, D. Gindre and B. Sahraoui, *Opt. Express*, 2012, **20**, 25311–25316.
31 P. Loiko, J. Bogusławski, J. M. Serres, E. Kifle, M. Kowalczyk, X. Mateos, J. Sotor, R. Zybała, K. Mars, A. MikuŁa, K. Kaszyca, M. Aguiló, F. Díaz, U. Griebner and V. Petrov, *Opt. Mater. Express*, 2018, **8**, 1723–1732.
32 M. Tuo, C. Xu, H. Mu, X. Bao, Y. Wang, S. Xiao, W. Ma, L. Li, D. Tang, H. Zhang, M. Premaratne, B. Sun, H.-M. Cheng, S. Li, W. Ren and Q. Bao, *ACS Photonics*, 2018, **5**, 1808–1816.
33 J. Fang, J. Wang, X. Cao, Y. Man, C. Liu, L. Cheng, X. Zhang, H. Zhao, H. Zhang and J. Li, *J. Phys. Commun.*, 2018, **2**, 015009.
34 Y. Wang, S. Liu, J. Yuan, P. Wang, J. Chen, J. Li, S. Xiao, Q. Bao, Y. Gao and J. He, *Sci. Rep.*, 2016, **6**, 33070.
35 Y. Jiang, Y. Ma, Z. Fan, P. Wang, X. Li, Y. Wang, Y. Zhang, J. Shen, G. Wang, Z.-J. Yang, S. Xiao, Y. Gao and J. He, *Opt. Lett.*, 2018, **43**, 523–526.
36 M. He, C. Quan, C. He, Y. Huang, L. Zhu, Z. Yao, S. Zhang, J. Bai and X. Xu, *J. Phys. Chem. C*, 2017, **121**, 27147–27153.
37 R. Chen, Y. Tang, X. Zheng and T. Jiang, *Appl. Opt.*, 2016, **55**, 10307–10312.
38 P. Li, Y. Chen, T. Yang, Z. Wang, H. Lin, Y. Xu, L. Li, H. Mu, B. N. Shivananju, Y. Zhang, Q. Zhang, A. Pan, S. Li, D. Tang, B. Jia, H. Zhang and Q. Bao, *ACS Appl. Mater. Interfaces*, 2017, **9**, 12759–12765.
39 J. Zhang, T. Jiang, T. Zhou, H. Ouyang, C. Zhang, Z. Xin, Z. Wang and X. Cheng, *Photonics Res.*, 2018, **6**, C8–C14.
40 I. Abdelwahab, P. Dichtl, G. Grinblat, K. Leng, X. Chi, I. Park, M. P. Nielsen, R. F. Oulton, K. P. Loh and S. A. Maier, *Adv. Mater.*, 2019, **31**, 1902685.
41 S. Zhang, N. Dong, N. McEvoy, M. O'Brien, S. Winters, N. C. Berner, C. Yim, Y. Li, X. Zhang, Z. Chen, L. Zhang, G. S. Duesberg and J. Wang, *ACS Nano*, 2015, **9**, 7142–7150.

